Current Biology *17*, 1146–1150, July 3, 2007  DOI 10.1016/j.cub.2007.05.072

Report

# Megafaunal Extinctions and the Disappearance of a Specialized Wolf Ecomorph

**Jennifer A. Leonard,[1,2,3] Carles Vilà,[3] Kena Fox-Dobbs,[4] Paul L. Koch,[4] Robert K. Wayne,[1] and Blaire Van Valkenburgh[1,*]**

[1] Department of Ecology and Evolutionary Biology
University of California
Los Angeles, California 90095

[2] Genetics Program and
Department of Vertebrate Zoology
National Museum of Natural History
Smithsonian Institution
Washington, D.C. 20008-0551

[3] Department of Evolutionary Biology
Uppsala University
75236 Uppsala
Sweden

[4] Department of Earth and Planetary Sciences
University of California
Santa Cruz, California 95064

## Summary

**The gray wolf (*Canis lupus*) is one of the few large predators to survive the Late Pleistocene megafaunal extinctions [1]. Nevertheless, wolves disappeared from northern North America in the Late Pleistocene, suggesting they were affected by factors that eliminated other species. Using skeletal material collected from Pleistocene permafrost deposits of eastern Beringia, we present a comprehensive analysis of an extinct vertebrate by exploring genetic (mtDNA), morphologic, and isotopic ($\delta\ ^{13}C$, $\delta\ ^{15}N$) data to reveal the evolutionary relationships, as well as diet and feeding behavior, of ancient wolves. Remarkably, the Late Pleistocene wolves are genetically unique and morphologically distinct. None of the 16 mtDNA haplotypes recovered from a sample of 20 Pleistocene eastern-Beringian wolves was shared with any modern wolf, and instead they appear most closely related to Late Pleistocene wolves of Eurasia. Moreover, skull shape, tooth wear, and isotopic data suggest that eastern-Beringian wolves were specialized hunters and scavengers of extinct megafauna. Thus, a previously unrecognized, uniquely adapted, and genetically distinct wolf ecomorph suffered extinction in the Late Pleistocene, along with other megafauna. Consequently, the survival of the species in North America depended on the presence of more generalized forms elsewhere.**

## Results

### Temporal Continuity

Radiocarbon dating of 56 ancient gray wolf specimens from permafrost deposits in Alaska shows a continuous population from 12,500 radiocarbon years before present (BP) to beyond the capacity of radiocarbon dating (Table S1 in the Supplemental Data available online). A single wolf was dated to 7,674 ± 66 BP (Figure S1). The near absence of wolves dated as younger than 12,500 BP likely reflects population decline rather than taphonomic bias because other extinct and extant megafauna (e.g., bison, elk, and moose) have been recovered from eastern Beringia dating between 12,500 and 10,000 BP [2].

### Genetic Relationships

To determine the relationship between ancient and modern Alaskan gray wolves, we successfully amplified the 5′ end of the mitochondrial control region and sequenced it in three overlapping fragments [3] from 20 ancient individuals, yielding 16 haplotypes. These sequences were compared to those from 436 recent wolves from throughout the world. None of the haplotypes identified in the ancient material was found in modern conspecifics. A phylogeny constructed with parsimony, maximum-likelihood, and distance approaches showed that the ancient American wolf haplotypes are generally basal to extant wolves (excluding Indian wolves), and no recent North American haplotypes clustered within them (Figure 1). Thus modern North American wolves are not their direct lineal descendents. Rather, nearly all modern Holarctic wolves share a common ancestry, whereas ancient North American wolves are phylogenetically associated with a distinct group of modern European haplotypes (lu5, lu6, lu15 and lu16), suggesting evolutionary turnover among wolves within North America. Genetic diversity of ancient wolves is also higher than that of their modern counterparts, implying that the population in the Late Pleistocene was larger than it is at present (Table S2).

The distinctness of the Pleistocene American wolves from recent American wolves is further supported by a comparison of our sequences of ancient eastern-Beringian wolves to much shorter 57 bp sequences of Pleistocene Old World wolves [4]. None of these ancient Old World sequences were identical to any modern wolf, and they differed from recent North American and European haplotypes by 1–10 bp (2%–18%). However, three (dated 30,000 BP and 28,000 BP from Ukraine, and 33,000 BP from Altai) had the same sequence found in six eastern-Beringian wolves (haplotypes PW1–PW4). Another haplotype from a 44,000 BP wolf from the Czech Republic matched those of two ancient Beringian wolves (haplotypes PW5 and PW9). This sequence identity between ancient Old World wolves and eight of the ancient eastern-Beringian wolves reaffirms the validity of our sequences and supports the existence of a separate origin for ancient and extant North American wolves.

### Craniodental Morphology

Skull measurements were taken from recent and Pleistocene gray wolves from Alaska and elsewhere in North

*Correspondence: bvanval@ucla.edu

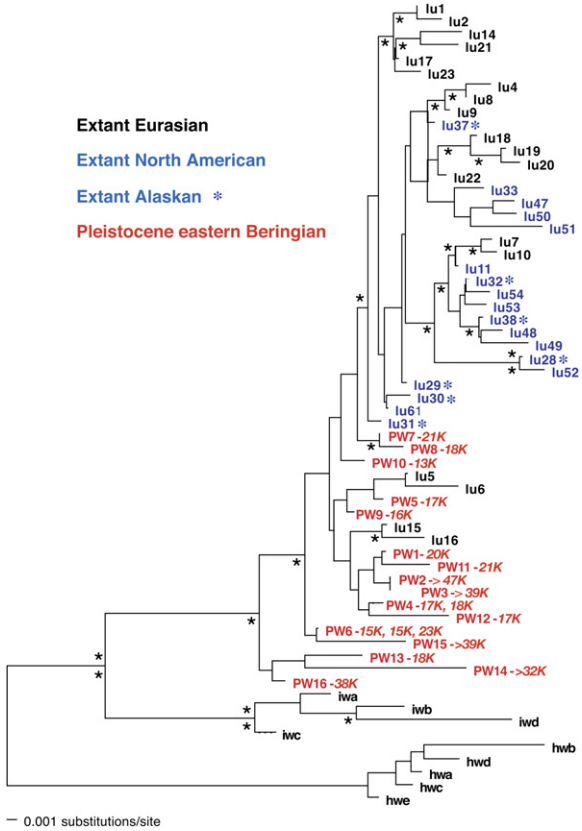


Figure 1. Neighbor-Joining Phylogeny of Pleistocene and Modern Wolves

Phylogeny based on 421–427 bp of mitochondrial control region I sequence (variation due to indels) rooted with Indian (iw) and Himalayan (hw) wolves [17]. Radiocarbon dates associated with each of the ancient haplotypes are listed in italics next to the relevant haplotype (K = thousand years BP). The bootstrap support for nodes in a neighbor-joining phylogeny (based on 1000 pseudoreplicates) and the percent of the 7200 most parsimonious trees when equal to or greater than 90% are indicated with an asterisk above and below nodes, respectively. Values for all support indices, including likelihood-reliability values, are available by request from the authors.

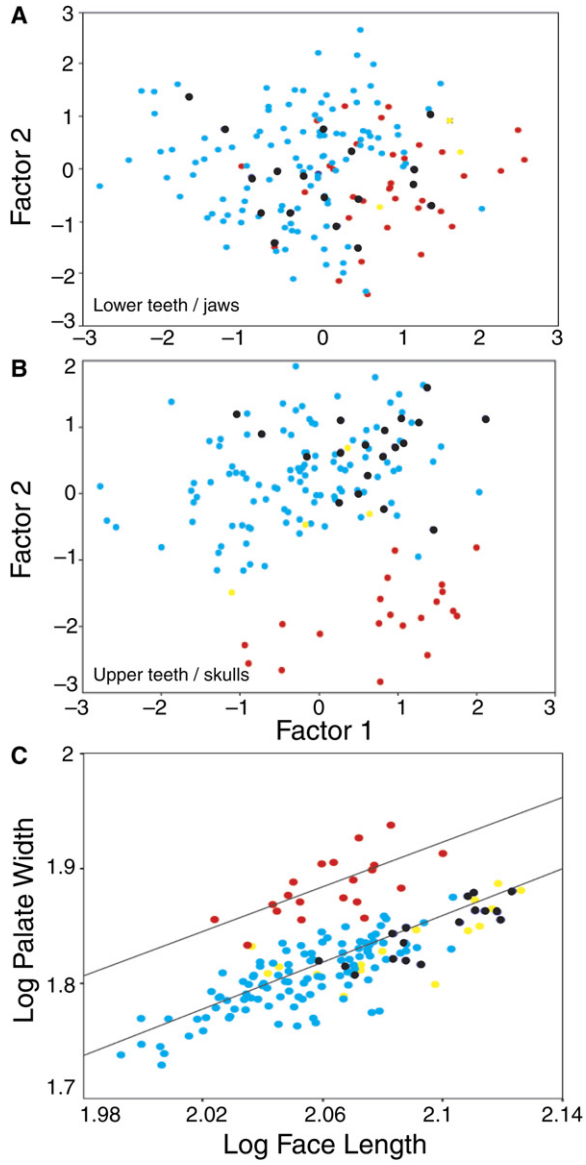


Figure 2. Plot of the First Two Factors of a PCA on $Log_{10}$-Transformed Shape Variables

(A and B) Dentary (A) and cranial (B) data.

(C) Linear regression of $\log_{10}$ palate width against $\log_{10}$ face length. The equation for the eastern-Beringian sample is the following: $\log_{10}$ PW = 0.928 · $\log_{10}$ FL -0.003; $r^2$ = 0.44. The equation for modern North American sample is the following: log PW = 0.906 · log FW - 0.005; $r^2$ = 0.64. The following symbols are used: Late Pleistocene eastern-Beringian wolves (red), La Brea wolves (yellow), modern Alaskan wolves (light blue), and non-Alaskan modern North American wolves (black).

America (Tables S3 and S4). Both analysis of variance (ANOVA) of the raw morphological data and principal components analysis (PCA) of geometric-mean-transformed shape variables (see Experimental Procedures) revealed that eastern-Beringian wolves differed significantly in shape from both the sample of modern North American wolves and Rancho La Brea (California) Pleistocene wolves (Figures 2A and 2B; Table S5). The disparity is more apparent for cranial than dentary shape, but Beringian wolves tend to cluster in a different space than other gray wolves in both plots of the first two PCA factors (Figures 2A and 2B). Cranial dimensions show almost no overlap (Figure 2B), with most of the separation occurring on the second PCA axis. Modern Alaskan and Pleistocene La Brea specimens overlap the distribution of other extant North American wolves, and they are distinct from the Pleistocene eastern-Beringian group. The Beringian wolves tend to have short, broad palates with large carnassials, relative to their overall skull size (Figure 2C; Tables S5 and S6).

Together, these features suggest a gray wolf adapted for producing relatively large bite forces. The short, broad rostrum increased the mechanical advantage of a bite made with the canine teeth and strengthened the skull against torsional stresses imposed by struggling prey [5, 6]. Relatively deep jaws are characteristic of habitual bone crackers, such as spotted hyenas (*Crocuta crocuta*) [7], as well as canids that take prey as large as or larger than themselves [8]. In all of these features, the eastern-Beringian wolves differed from

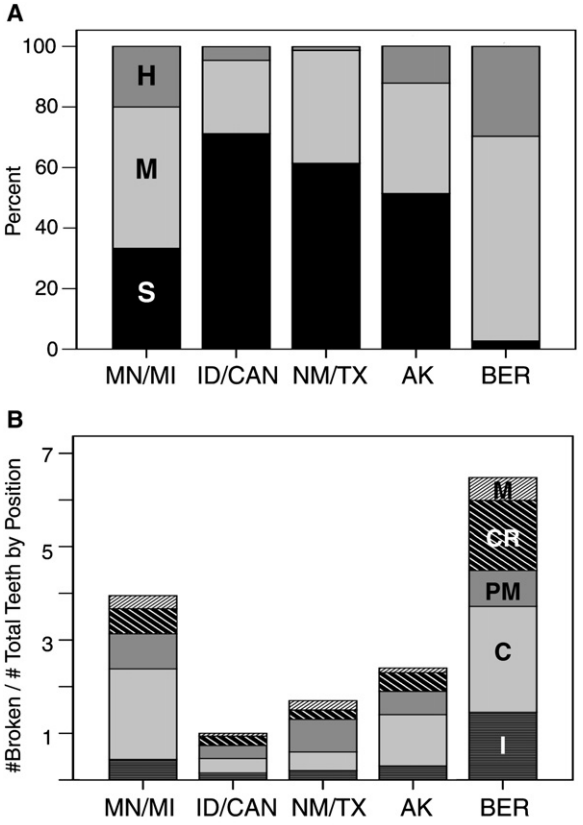


Figure 3. Tooth Wear Data from Five Gray Wolf Samples

(A) Percent of individuals in each wear-stage category. The following abbreviations are used: slight (S), moderate (M), and heavy (H), as indicated in the leftmost bar.

(B) Percentage of broken teeth for each tooth type. The following abbreviations are used: incisors (I) canines (C), premolars (PM), carnassials (CR), and molars (M), as indicated in the rightmost bar. The following sample labels are used: Minnesota and Michigan (MN/MI), Idaho and adjacent Canada (ID/CAN), New Mexico and Texas (NM/TX), Alaska (AK), and Late Pleistocene eastern Beringia (BER). For sample sizes, see Table S7.

their extant counterparts and Pleistocene Rancho La Brea gray wolves in a direction that suggests greater specialization for killing and consuming relatively large prey and/or habitual scavenging.

### Tooth Wear and Fracture

All eastern-Beringian wolves used in the morphometric analysis and 313 modern, wild-caught, adult wolves from four North American subspecies (Table S7) were scored for overall tooth wear (slight, moderate, and heavy; see Experimental Procedures). In addition, the number and position of teeth broken in life were recorded for each individual. Relative to modern populations from a range of environments (Alaska to Arizona), the sample of Beringian wolves includes many more individuals with moderately and heavily worn teeth (97%; Figure 3A). In addition, eastern-Beringian gray wolves exhibit heavier wear and significantly greater numbers of broken teeth. Overall fracture frequencies ranged from a low of 2% in *C. lupus irremotus* (Canada, Idaho) to a high of 11% in the Pleistocene eastern-Beringian wolves (Table S7). The distribution of fractures across the tooth row differs as well, with eastern-Beringian wolves having much higher fracture frequencies of incisors, carnassials, and molars (Figure 3B). A similar pattern was observed for spotted hyenas, relative to those of canids (including gray wolves) and felids [9], suggesting that increased incisor and carnassial fracture reflects habitual bone consumption because bones are gnawed with incisors and subsequently cracked with cheek teeth.

### Stable Isotopes

Stable isotope ($\delta\,^{13}C$ and $\delta\,^{15}N$) data were collected from bone collagen of Late Pleistocene wolves (n = 40) and their potential prey, including horses (*Equus lambei*), caribou *(Rangifer tarandus*), bison (*Bison bison*), yak (*Bos grunniens*), and woodland muskox (*Symbos cavifrons*) (Table S8). We also included published $\delta\,^{13}C$ and $\delta\,^{15}N$ data collected from undated Pleistocene mammoths (*Mammuthus primigenius)* from multiple sites in Alaska [10]. To eliminate potential isotopic variability among individuals due to spatial differences, we obtained all samples (except mammoth) from the Fairbanks area. The $\delta\,^{13}C$ values of Beringian wolves range from −18.3‰ to −20.5‰, and $\delta\,^{15}N$ values range from 10.3‰ to 5.4‰ (excluding one outlying full-glacial individual with a value of 12.7‰) (Table S8). All preglacial and postglacial wolf values (corrected for trophic-level isotopic enrichments) fall within a dietary isospace defined by megafaunal prey $\delta\,^{13}C$ and $\delta\,^{15}N$ values (Figure 4). Two full-glacial wolves have high $\delta\,^{13}C$ or $\delta\,^{15}N$ values that seem difficult to explain with existing prey values, but we do not have a large sample of full-glacial caribou, and this might better explain these deviant values. The variances of wolf $\delta\,^{13}C$ values are similar among time periods (Levene's test; F = 0.4, p = 0.65), whereas those of $\delta\,^{15}N$ values differ significantly (Levene's test; F = 4.9, p = 0.013), with postglacial wolves being less variable than preglacial and full-glacial wolves. If the outlier with a very high $\delta\,^{15}N$ value (12.7‰) is removed, the difference between full-glacial and postglacial samples is no longer significant, but the preglacial sample remains significantly more variable than do the younger samples (Levene's test; F = 8.8, p = 0.0008). In each of the three time periods, isotope values from wolves are intermediate among prey types, suggesting that they had diets comprised of a mix of species. Horse and bison appear to have been prey for wolves during all three time periods, whereas woodland muskox show up in the wolves' diets only in preglacial times, and mammoth seems to have been consumed only after this time. Thus, eastern-Beringian wolves as a group preyed on a wide diversity of species, including megafauna that are now extinct, supporting the conclusion of the morphologic analysis that they were capable of killing and dismembering large prey.

### Discussion

Our morphological and isotopic data demonstrate the existence of a previously undetected ecomorph of the gray wolf in the Late Pleistocene of eastern Beringia and suggest an evolutionary plasticity of craniodental form within *C. lupus* greater than previously observed in modern North American gray wolves. This wolf was

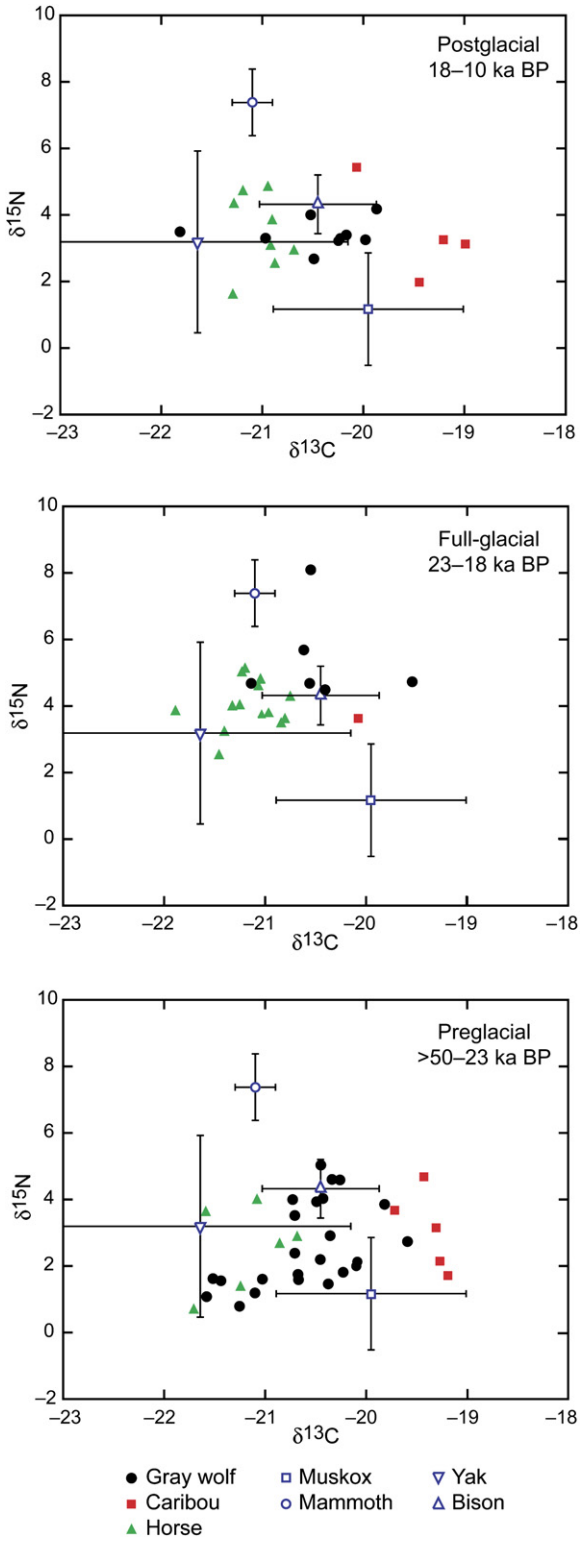


Figure 4. Dietary Reconstructions for Late Pleistocene Gray Wolves from the Fairbanks Region

In each reconstruction, the wolf $\delta^{13}C$ and $\delta^{15}N$ values have been corrected for trophic-level isotopic fractionation (−1.3‰ for $\delta^{13}C$, and −4.6‰ for $\delta^{15}N$) and are compared to isotope values of megafaunal prey species from the Fairbanks area (except for mammoth, which are from sites throughout Alaska). Horse and caribou individuals were $^{14}C$ dated, and discrete isotopic values are included for individuals from each time period. Bison, yak, muskox, and mammoth were not $^{14}C$ dated, and a range of isotopic values (means ± standard deviations) are included for each time period. Mammoth isotopic data are from reference [10].

similar in size to coeval Rancho La Brea wolves and modern Alaskan wolves, but it had stronger jaws and teeth. Moreover, tooth fracture frequency was high (11%) and comparable to that observed among four large Pleistocene predators from south of the ice sheets [11]—from 7% in dire wolves (*Canis dirus*), coyotes (*C. latrans*), and saber-toothed cats (*Smilodon fatalis*), to 17% in American lions (*Panthera atrox*). The greater tooth fracture in Pleistocene carnivores suggests heavier carcass utilization in the past, probably as a result of higher carnivore densities and increased competition. This same explanation could apply to the eastern-Beringian gray wolves because they coexisted with several formidable predators, including the American lion, short-faced bear (*Arctodus simus*), brown bear (*Ursus arctos*), scimitar-tooth sabercat (*Homotherium serum*), and dhole (*Cuon alpinus*).

Compared with extant gray wolves and Pleistocene gray wolves from Rancho La Brea, the eastern-Beringian ecomorph was hypercarnivorous with a craniodental morphology more capable of capturing, dismembering, and consuming the bones of very large mega-herbivores, such as bison. When their prey disappeared, this wolf ecomorph did as well, resulting in a significant loss of phenotypic and genetic diversity within the species. Conceivably, the robust ecomorph also was present in western Beringia in the Late Pleistocene, but specimens were not available for this study.

A plausible scenario for the presence of two distinct Pleistocene gray wolves in North America relies on an early arrival of the more gracile wolf from the Old World and migration to areas below the Wisconsin ice sheet. This gray wolf insinuated itself into a carnivore guild that already contained forms both larger (dire wolf) and smaller (coyote) than itself. The presence of these two relatively common species (especially the dire wolf) seems to have prevented gray wolves from reaching high densities until after the demise of the dire wolf, approximately 10 ka BP [12]. The appearance of a more robust form of the gray wolf in eastern Beringia in the Late Pleistocene might represent evolution in situ or a secondary invasion from the Old World. Its success was favored by the absence of dire wolves north of the ice sheet [12]. Otherwise, the eastern-Beringian gray wolf would probably not have evolved in the same direction as the dire wolf, acquiring a more robust skull and dentition, because that would have increased ecological overlap between the two species. Instead, the eastern-Beringian gray wolf was well positioned as the dominant large, pack-hunting canid within a predator guild that included large felids, ursids, and two smaller canids, the dhole and coyote [1].

Greater extinction vulnerability of relatively specialized forms has been shown for other Pleistocene carnivores [13]. Species that did not survive were usually the largest and most carnivorous within their family. Among the felids, the large lion and saber tooth disappeared, whereas the relatively eurytopic puma and bobcat (*Lynx rufus*) survived. Among the bears, the species with the greatest dental specialization for carnivory, the

short-faced bear, vanished, but the more omnivorous and smaller black (*Ursus americanus*) and brown bears remain [13]. Similarly, the dire wolf was lost, whereas the smaller gray wolf and coyote survived. However, the gray wolf did not survive unscathed—we show that at least one ecologically distinct form was lost and replaced by a smaller and more generalized form. Past studies of Pleistocene survivors [14–16] also demonstrated a loss of genotypic diversity but did not explore changes in morphologic diversity. Thus, there may be other extinctions of unique Pleistocene ecomorphs yet to be discovered.

### Experimental Procedures

Details of the experimental procedures are given in the Supplemental Data. Our eastern-Beringian gray wolf sample was restricted to specimens positively identified as *Canis lupus* and a few specimens of uncertain identity (labeled "*Canis sp.*") that were radiocarbon dated as greater than 7 ka BP (to eliminate to the possibility of recent wolves and dogs) (Table S1). Specimens are from the collections of the American Museum of Natural History (AMNH) (New York) and the Canadian Museum of Nature (CMN) (Ottawa, Canada). We also examined the morphology of a sample (n = 15) of gray wolves from the Pleistocene Rancho La Brea tar seeps of California that are in the collections of the Natural History Museum of Los Angeles County (LACM). All specimens used in the analyses are listed in Table S1, along with radiocarbon dates when available.

### Supplemental Data

Experimental Procedures, one figure, and eight tables are available at http://www.current-biology.com/cgi/content/full/17/13/1146/DC1/.

### Acknowledgments

We thank R. Fisher (United States National Museum [USNM]), R. Harington (CMN), R. Tedford (AMNH), C. Shaw (LACM), and J.M. Harris (LACM) for access to specimens for biochemical and morphological analyses. For assistance with radiocarbon dating, we thank T. Guilderson at the Center for Accelerator Mass Spectrometry, Lawrence Livermore National Laboratory. Logistical support was provided by the Genetics Program, National Museum of Natural History, Smithsonian Institution. K. Koepfli provided very useful assistance and advice with molecular and phylogenetic analyses. This work was funded by the National Science Foundation OPP 9817937 (R.K.W. and B.V.V), OPP 0352634 (R.K.W., J.A.L., and P.L.K.), and the Swedish Research Council (J.A.L. and C.V.).

Received: April 12, 2007
Revised: May 25, 2007
Accepted: May 29, 2007
Published online: June 21, 2007

### References

1. Kurten, B., and Anderson, E. (1980). Pleistocene Mammals of North America (New York: Columbia University Press).
2. Guthrie, R.D. (2006). New carbon dates link climatic change with human colonization and Pleistocene extinctions. Nature *441*, 207–209.
3. Leonard, J., Wayne, R.K., Wheeler, J., Valadez, R., Guillén, S., and Vilà, C. (2002). Ancient DNA evidence for Old World origin of New World dogs. Science *298*, 1613–1616.
4. Stiller, M., Green, R.E., Ronan, M., Simons, J.F., Du, L., He, W., Egholm, M., Rothberg, J.M., Keats, S.G., Ovodov, N.D., et al. (2006). Patterns of nucleotide misincorporations during enzymatic amplification and direct large-scale sequencing of ancient DNA. Proc. Natl. Acad. Sci. USA *103*, 13578–13584.
5. Biknevicius, A., and Van Valkenburgh, B. (1996). Design for killing: Craniodental adaptations of predators. In Carnivore Behavior, Ecology, and Evolution, *Vol. II*, J.L. Gittleman, ed. (Ithaca, New York: Cornell University Press), pp. 393–428.
6. Covey, D.S.G., and Greaves, W.S. (1994). Jaw dimensions and torsion resistance during canine biting in the Carnivora. J. Zool. *72*, 1055–1060.
7. Biknevicius, A.R., and Ruff, C.B. (1992). The structure of the mandibular corpus and its relationship to feeding behaviors in extant carnivorans. J. Zool. *228*, 479–507.
8. Van Valkenburgh, B., and Koepfli, K. (1993). Cranial and dental adaptations for predation in canids. In Mammals as Predators, N. Dunstone and M.L. Gorman, eds. (Oxford: Oxford University Press), pp. 15–37.
9. Van Valkenburgh, B. (1988). Incidence of tooth breakage among large, predatory mammals. Am. Nat. *131*, 291–302.
10. Bocherens, H., Fizet, M., Mariotti, A., Gangloff, R.A., and Burns, J.A. (1994). Contribution of isotopic biogeochemistry (13C, 15N, 18O) to the paleoecology of mammoths (*Mammuthus primigenius*). Historical Biology *7*, 187–202.
11. Van Valkenburgh, B., and Hertel, F. (1993). Tough times at La Brea: Tooth breakage in large carnivores of the late Pleistocene. Science *261*, 456–459.
12. Dundas, R.G. (1999). Quaternary records of the dire wolf, Canis dirus, in North and South America. Boreas *28*, 375–385.
13. Van Valkenburgh, B., and Hertel, F. (1998). The decline of North American predators during the Late Pleistocene. In Quaternary Paleozoology in the Northern Hemisphere, *Volume 27*, J.J. Saunders, B.W. Styles, and G.F. Baryshnikov, eds. (Springfield, Illinois: Illinois State Museum Scientific Papers), pp. 357–374.
14. Barnes, I., Matheus, P., Shapiro, B., Jensen, D., and Cooper, A. (2002). Dynamics of Pleistocene population extinctions in Beringian brown bears. Science *295*, 2267–2270.
15. Leonard, J., Wayne, R., and Cooper, A. (2000). Population genetics of ice age brown bears. Proc. Natl. Acad. Sci. USA *97*, 1651–1654.
16. Shapiro, B., Drummond, A.J., Rambaut, A., Wilson, M.C., Matheus, P.E., Sher, A.V., Pybus, O.G., Gilbert, M.T.P., Barnes, I., Binladen, J., et al. (2004). Rise and fall of the Beringian steppe bison. Science *306*, 1561–1565.
17. Sharma, D.K., Maldonado, J.E., Jhala, Y.V., and Fleischer, R.C. (2003). Ancient wolf lineages in India. Proc. R. Soc. Lond. B. Biol. Sci. *271*, S1–S4.

# Supplemental Data



# Megafaunal Extinctions and the Disappearance of a Specialized Wolf Ecomorph

**Jennifer A. Leonard, Carles Vilà, Kena Fox-Dobbs, Paul L. Koch, Robert K. Wayne, and Blaire Van Valkenburgh**

## Supplemental Experimental Procedures

### Genetic Analysis

DNA was extracted from tooth and bone samples by phenol-chloroform extraction as in Leonard et al. [S1]. Two blank (no bone powder) extractions were processed concurrently throughout all steps of the protocol to serve as negative controls. Approximately 425 bp of mitochondrial control region I was amplified in three overlapping regions with the following primers: Thr-L 5′-GAATTCCCC GGTCTTGTAAACC-3′ and dogdl5 5′-CATTAATGCACGACGTACA TAGG-3′ (yielded polymerase chain reaction [PCR] products of 207–227 bp in length); dogdl1g 5′-GTGCTATGTCAGTATCTCCA GG-3′ and dogdl2 5′-GCAAGGGTTGATGGTTTCTCG-3′ (235 bp); and dogdl4 5′-GCATATCACTTAGTCCAATAAGGG-3′ and DLH-can 5′-CCTGAGGTAAGAACCAGATG-3′ (150 bp) as in Leonard et al. [S1]. The setup for PCR amplification of DNA was performed in a separate lab exclusively devoted to ancient-DNA extraction, and each reaction consisted of 3–6 μl of extract and 25 ng bovine serum albumin (BSA), 1X buffer, 0.1 mM deoxyribonucleotide triphosphate (dNTP), 2.5 U AmpliTaq Gold (Perkin-Elmer), 2.5 mM $Mg^{2+}$, and 2.5 μM each primer in a total volume of 25 μl. The product of each successful reaction was either directly sequenced or used as a source for reamplification, and this product was then sequenced.

PCR products were purified with the UltraClean kit (MoBio, Carlsbad, California). Products were cycle-sequenced in a Primus 96 plus (MWG-Biotech, High Point, North Carolina) PCR instrument with BigDye terminator (Perkin-Elmer, Boston) chemistry. Sequences were then separated on an Applied Biosystems automated sequencer 377 according to the manufacturer's protocols. The same primers were used for both PCR and sequencing. Fragments were sequenced in both directions.

Precautions for analysis of low-copy DNA include nucleic-acid isolation in a pre-PCR ancient-DNA facility separated from the PCR-amplification laboratory by five floors and two corridors, as well as replications as in Leonard et al. [S1]. The ancient-DNA lab utilized ultraviolet lights to inactivate DNA, had an independent air-handling system with hepa filters on all vents, and was under positive air displacement. Two PCR blanks, as well as both extraction blanks, were run with each PCR reaction to monitor for contamination. We used three different sets of PCR primers to produce overlapping sequences that could be compared to detect contamination. Further, 80% of the sequences were confirmed independently by amplification and sequencing multiple times. No canid contamination was detected [S2].

The eastern-Beringian wolf sequences were compared with those of 32 modern wolves from Alaska and the Yukon, as well as with previously reported sequences from 401 recent wolves throughout the world [S3–S5]. Nucleotide and haplotype diversity, as well as their standard deviations, were calculated with DnaSP 4.10.9 [S6]. Three different criteria were used to construct phylogenies (maximum parsimony, maximum likelihood, and distance-based neighbor joining) in the program PAUP* 4.0b10 [S7]. Himalayan and Indian wolves were used as outgroups in all analyses [S5]. For the parsimony analysis, a heuristic search including indels as fifth state was run, and a consensus tree of all of the most parsimonious trees was constructed. The model of sequence evolution which best fit the data was estimated in ModelTest [S8] and used in the likelihood and distance analyses. The best-fit model was the HKY85 with a γ parameter (G = 0.9082) and a portion of invariant sites (I = 0.5213). For the likelihood analysis, the puzzle quartet algorithm was used and reliability values were estimated. Lastly, for the distance analysis, a neighbor-joining phylogeny was constructed, and bootstrap support for branches was estimated with 1000 pseudoreplications.

### Morphological Analysis

Twenty-seven craniodental measurements were taken by J.A.L. and C.V. with digital calipers on 116 modern-wolf skulls from North America, ranging from Ellesmere Island, Canada to northern Mexico (Table S3). All were adult wild-caught individuals in the mammal collections of the American Museum of Natural History (AMNH) or the National Museum of Natural History (USNM). Specimen numbers are available from the authors on request. In addition, data were collected from 35 crania and 37 dentaries of Pleistocene wolves (Table S3). Most of the Pleistocene specimens are incomplete, and dentaries are not usually associated with crania, so the two skull parts were analyzed separately. Moreover, because of their fragmentary nature, only a subset of measurements was possible. To maximize the sample of Pleistocene wolves used in statistical analyses, the number of measurements was reduced to 11 for the skull and upper teeth and seven for the lower jaw and teeth (Table S4). With the software SPSS 11 for Mac OS X, measurements were subjected to bivariate and multivariate analyses, including analysis of variance (ANOVA), principal components analysis (PCA), and linear regression. The ANOVA tested for significant differences in single measures between the ancient and modern populations of wolves. For better identification of shape differences among wolves, PCA was performed on size-transformed data, with Mosimann shape variables [S9, S10]. Each of the raw measures was divided by the geometric mean (GM), which is defined as the $n^{th}$ root of the product of n raw measurements. For the minimization of the effect of outliers, ratios were $\log_{10}$ transformed prior to entry into the PCA. For testing for remaining correlations between shape variables and size, correlations between principal component scores on the first two axes and size were determined with the $\log_{10}$ of the GM as an overall estimate of body size.

### Tooth-Wear Analysis

All eastern-Beringian wolves used in the morphometric analysis and 313 modern, wild-caught, adult wolves from four subspecies were examined for tooth wear and fracture by B.V.V. (Tables S1 and S7). The modern-wolf skulls are part of the USNM mammal collection.

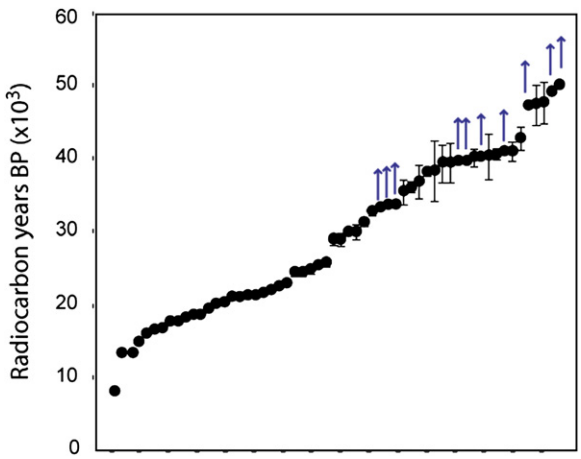


Figure S1. Radiocarbon Dates for 58 *Canis lupus* from East-Beringian Permafrost Deposits

Arrows indicate specimens with infinite dates. Specimens are from the AMNH and NMC collections of Pleistocene mammals (Table S1).

Table S1. Fossil Wolf Specimens Included in the Study, Mitochondrial DNA Haplotypes Identified, and Their Uncalibrated Radiocarbon Dates, if Available

| Specimen Number | Species | Element | DNA | DATE | Lab # |
|---|---|---|---|---|---|
| AMNH FM 68008-6# | *Canis lupus* | ulna | PW6 | 23,380 ± 470 | AA35222 |
| AMNH FM 30447# | *"C. lupus"* | femur | | 15,680 ± 190 | AA35223 |
| AMNH FM 67224*# | *"C. lupus"* | ramus | PW4 | 17,640 ± 240 | AA35226 |
| AMNH FM 58009-A# | *"C. lupus"* | femur | PW12 | 16,800 ± 210 | AA35227 |
| AMNH FM 67240# | *"C. lupus"* | ramus | PW13 | 28,610 ± 860 | AA35228 |
| AMNH FM 67199*# | *"C. lupus"* | ramus | PW8 | 18,380 ± 390 | AA35230 |
| AMNH FM 67227*# | *"C. lupus"* | ramus | PW9 | 15,870 ± 190 | AA35231 |
| AMNH FM 70958# | *"C. lupus"* | ramus | | 37,700 ± 2600 | AA37615 |
| AMNH FM 67212# | *Canis sp.* | ramus | | | |
| AMNH FM 67208* | *"C. lupus"* | ramus | | 41,040 ± 1530 | CAMS 115759 |
| AMNH FM 67204* | *"C. lupus"* | ramus | | | |
| AMNH FM 67179* | *"C. lupus"* | ramus | | 36,700 ± 4000 | AA37617 |
| AMNH FM 67197* | *"C. lupus"* | ramus | | 39,300 ± 1230 | CAMS 115760 |
| AMNH FM 67216# | *"C. lupus"* | ramus | PW5 | 17,330 ± 290 | AA42301 |
| AMNH FM 30480* | *"C. lupus"* | ramus | | | |
| AMNH FM 67228# | *C. lupus* | ramus | PW14 | >32,100 | AA42302 |
| AMNH FM 67203*# | *"C. lupus"* | ramus | PW15 | >39,200 | AA42303 |
| AMNH FM 67207* | *C. lupus* | ramus | | | |
| AMNH FM 67202# | *"C. lupus"* | ramus | | 38,000 ± 2,700 | AA35224 |
| AMNH FM 67230* | *"C. lupus"* | ramus | | | |
| AMNH FM 30438*# | *"C. lupus"* | cranium | | 45,500 ± 2700 | CAMS 115778 |
| AMNH FM 67235*# | *"C. lupus"* | ramus | | >38,000 | AA42310 |
| AMNH FM 70945*# | *"C. lupus"* | ramus | PW16 | 37,733 ± 2633 | AA38448 |
| AMNH FM 70944*# | *"C. lupus"* | ramus | PW6 | 15,268 ± 169 | AA38449 |
| AMNH FM 142411 | *"C. lupus"* | humerus | | 24,130 ± 190 | CAMS 115761 |
| AMNH FM 142410 | *"C. lupus"* | humerus | | >45,400 | CAMS 115762 |
| AMNH FM 67184 | *"C. lupus"* | ramus | | 34,600 ± 700 | CAMS 115763 |
| AMNH FM 30476# | *"C. lupus"* | ramus | | 20,050 ± 430 | AA42312 |
| AMNH FM 70946*# | *"C. lupus"* | ramus | PW3 | >38,570 | AA42313 |
| AMNH FM 30440*# | *"C. lupus"* | ramus | | >38,000 | AA42314 |
| AMNH FM 67256* | *"C. lupus"* | ramus | | | |
| AMNH FM 67250* | *"C. lupus"* | ramus | | | |
| AMNH FM 30477* | *"C. lupus"* | ramus | | | |
| AMNH FM 67210* | *"C. lupus"* | ramus | | | |
| AMNH FM 68006-I# | *Canis sp.* | humerus | | | |
| AMNH FM 30445# | *Canis sp.* | humerus | | | |
| NMC 42388# | *C. lupus* | | | 33,900 ± 1700 | AA35221 |
| AMNH FM 97079* | *C. lupus* | cranium | | 23,660 ± 490 | AA48690 |
| AMNH FM 30430* | *C. lupus* | cranium | | 19,280 ± 290 | AA48691 |
| AMNH FM 67160* | *C. lupus* | cranium | | 24,630 ± 520 | AA48692 |
| AMNH FM 67163* | *C. lupus* | cranium | | >31,800 | AA48693 |
| AMNH FM 67170* | *C. lupus* | cranium | | 27,620 ± 580 | AA48694 |
| AMNH FM 67169*# | *C. lupus* | ramus | | 20,305 ± 385 | |
| AMNH FM 97079# | *C. lupus* | ramus | | >32,100 | |
| AMNH FM 30450*# | *C. lupus* | cranium | | 7,674 ± 66 | AA48695 |
| AMNH FM 30433* | *C. lupus* | cranium | | 12,690 ± 130 | AA48697 |
| AMNH FM 30457* | *C. lupus* | cranium | | 38,600 ± 3000 | AA48698 |
| AMNH FM 67162* | *C. lupus* | cranium | | 23,230 ± 440 | AA48700 |
| AMNH FM 67168*[a] | *C. lupus* | cranium | | 27,690 ± 790 | AA48701 |
| AMNH FM 67168*[a] | *C. lupus* | cranium | | 31,200 ± 450 | CAMS 115767 |
| AMNH FM 30453* | *C. lupus* | cranium | | 19,210 ± 260 | AA48702 |
| AMNH FM 30458* | *C. lupus* | cranium | | | |
| AMNH FM 67158* | *C. lupus* | cranium | | | |
| AMNH FM 67159* | *C. lupus* | cranium | | 35,200 ± 2300 | AA48703 |
| AMNH FM 70935* | *C. lupus* | cranium | | | |
| AMNH FM 30432* | *C. lupus* | cranium | | 17,670 ± 230 | AA48704 |
| AMNH FM 67167* | *C. lupus* | cranium | | 45,800 ± 2800 | CAMS 115768 |
| AMNH FM 67166* | *C. lupus* | cranium | | | |
| AMNH FM 30431* | *C. lupus* | cranium | | 28,500 ± 300 | CAMS 115776 |
| AMNH FM 30452* | *C. lupus* | cranium | | 20,550 ± 120 | CAMS 115769 |
| AMNH FM 67164* | *C. lupus* | cranium | | | |
| AMNH FM 67211* | *"C. lupus"* | ramus | | | |
| AMNH FM 67201* | *C. lupus* | ramus | | | |
| AMNH FM 67194* | *C. lupus* | ramus | | | |
| AMNH FM 67209* | *C. lupus* | ramus | | | |
| AMNH FM 67243* | *C. lupus* | ramus | | 38,500 ± 1,100 | CAMS 115772 |
| AMNH FM 67182* | *C. lupus* | ramus | | | |
| AMNH FM 30478* | *C. lupus* | ramus | | | |
| AMNH FM 67248* | *C. lupus* | ramus | | 29,800 ± 400 | CAMS 115773 |

Table S1. *Continued*

| Specimen Number | Species | Element | DNA | DATE | Lab # |
|---|---|---|---|---|---|
| AMNH FM 67231* | *C. lupus* | ramus | | 21,900 ± 140 | CAMS 115774 |
| AMNH FM 67239* | *"C. lupus"* | ramus | | | |
| AMNH FM 70951* | *"C. lupus"* | ramus | | | |
| AMNH FM 70943* | *"C. lupus"* | ramus | | | |
| AMNH FM 70942* | *C. lupus* | ramus | | 20,150 ± 110 | CAMS 115775 |
| AMNH FM 70950* | *"C. lupus"* | ramus | | | |
| AMNH FM 67169# | *"C. lupus"* | cranium | PW1 | 20,305 ± 385 | AA35216A |
| AMNH FM 67165*# | *C. lupus* | cranium | PW10 | 12,600 ± 150 | AA42317 |
| AMNH FM 67157*# | *C. lupus* | cranium | PW6 | 14,030 ± 50 | UCR 3760 |
| AMNH FM 30451*# | *C. lupus* | cranium | PW4 | 16,800 ± 90 | UCR 3761 |
| NMC 17311# | *C. lupus* | cranium | PW17 | 38,780 ± 540 | UCR 3762 |
| NMC 45574# | *C. lupus* | cranium | PW11 | 21,490 ± 110 | UCR 3763 |
| NMC 9929# | *C. lupus* | cranium | PW7 | 20,920 ± 70 | UCR 3764 |
| NMC CR-95100# | *C. lupus* | cranium | PW2 | >47,170 | Beta 89988 |
| NMC 44726# | *C. lupus* | humerus | | 36,490 ± 410 | UCR 3765 |
| LACM 1414* | *C. lupus* | cranium | | | |
| LACM 314* | *C. lupus* | cranium | | | |
| LACM hc606* | *C. lupus* | cranium | | | |
| LACM 615* | *C. lupus* | cranium | | | |
| LACM 2300-384* | *C. lupus* | cranium | | | |
| LACM 2600* | *C. lupus* | cranium | | | |
| LACM HC607* | *C. lupus* | cranium | | | |
| LACM2300-353* | *C. lupus* | cranium | | | |
| LACM 2600-2* | *C. lupus* | cranium | | | |
| LACM 604* | *C. lupus* | cranium | | | |
| LACM 609* | *C. lupus* | cranium | | | |
| LACM 11505* | *C. lupus* | cranium | | | |
| LACM 608* | *C. lupus* | cranium | | | |
| LACM 6909* | *C. lupus* | cranium | | | |
| LACM 11505* | *C. lupus* | cranium | | | |

Specimens used in the morphological and/or tooth fracture analyses are indicated by an asterisk. Specimens used in the genetic analyses are indicated by the pound sign, and those which yielded complete sequences have the haplotype indicated in the "DNA" column. Specimens listed as *"C. lupus"* were labeled as *Canis sp.* in the collection but considered to be *C. lupus* by R.H. Tedford on the basis of craniodental morphology. The following museum abbreviations are used: Frick Collection of the American Museum of Natural History, New York (AMNH FM); Museum of Natural History of Los Angeles County collections of the George C. Page Museum, Los Angeles (LACM); and Nature Museum of Canada, Ottawa (NMC). "Lab #" indicates the catalogue number at the radiocarbon-dating laboratory. Radiocarbon dating was done at Arizona Accelerator Mass Spectrometry Laboratory (AA), University of California, Riverside Radiocarbon Laboratory (UCR), Beta Analytic (Beta), and Center for Accelerator Mass Spectrometry, Lawrence Livermore National Laboratory (CAMS).

[a] These two specimens are partial skulls with the same catalog number but different field numbers.

As in previous studies of tooth-fracture frequency [S11, S12], each individual was scored for overall wear as one of three stages: (1) *slight*, little or no apparent wear observed as shear facets or blunting of cusps; (2) *moderate*, shear facets apparent on carnassial teeth, and cusps blunted on most teeth; or (3) *heavy,* carnassial teeth with strong shear facets or blunted cusps, and premolars and molars with well-rounded cusps. The number and identity of teeth broken in life were recorded for each individual. A tooth was counted as broken in life only if it exhibited wear that must have occurred after fracture. Total fracture frequency was calculated as a weighted average of tooth fracture frequencies for each tooth type (incisors, canines, premolars, carnassial, and molars) [S11]. The weighted average was used because the relative representation of tooth types (e.g., incisors) often differs between fossil and modern samples

Table S2. Nucleotide and Haplotype Diversity of North American Gray Wolf Populations

| Population | n | Haplotype Diversity | Nucleotide Diversity |
|---|---|---|---|
| Pleistocene | 19 | 0.977 ± 0.027 | 0.0125 ± 0.0021 |
| Pleistocene, 12–18K bp only | 10 | 0.956 ± 0.059 | 0.0103 ± 0.0026 |
| Recent Alaska | 29 | 0.791 ± 0.038 | 0.0093 ± 0.0008 |
| Recent Inuvik | 40 | 0.595 ± 0.085 | 0.0044 ± 0.0008 |
| Recent *C. l. nubilus*[a] | 22 | 0.831 ± 0.054 | 0.0135 ± 0.0012 |

Pleistocene populations are from eastern Beringia, and the 12–18 ka BP population is a subset of the entire Pleistocene population. The number of samples used to calculate the haplotype and nucleotide diversities is indicated in the column labeled "n." Each haplotype- and nucleotide-diversity value is followed by its standard deviation. The genetic diversity of Pleistocene wolves is higher than that of their modern counterparts. We find 16 haplotypes in 20 ancient Beringian wolves, compared with only seven haplotypes in a sample of 32 modern Alaska and Yukon wolves. The sample of ancient wolves represents a time-averaged sample that might increase the apparent genetic diversity. However, even in a narrow time range of 12 to 18 thousand years before present we find eight haplotypes in 10 wolves from a single locality, a higher diversity than that in any modern North American population. Assuming that the populations were at demographic equilibrium, such differences in genetic diversity would imply that the ancient-wolf population was larger than that of the current day, and might have been so for some time.

[a] Historic wolves from the contiguous United States.

Table S3. Sample of Pleistocene *Canis lupus* and Subspecies of Extant *C. lupus* Measured

| Population | n (crania) | n (dentaries) | Provenance |
|---|---|---|---|
| *C. lupus* (Pleistocene) | 20 | 34 | Alaska |
| *C. lupus* (Pleistocene) | 15 | 3 | California (Rancho La Brea) |
| *C. l. baileyi* | 9 | 10 | Mexico, New Mexico |
| *C. l. lycaon* | 22 | 24 | Eastern Canada, Minnesota, Michigan |
| *C. l. mongollensis* | 12 | 11 | Arizona, New Mexico |
| *C. l. monstrabilis* | 10 | 9 | Mexico, New Mexico, Texas |
| *C. l. nubilus* | 26 | 26 | Texas, Nebraska, Colorado, Kansas. Oklahoma, South Dakota |
| *C. l. youngi* | 12 | 12 | Colorado, New Mexico, Utah, Wyoming |
| *C. l. pambasileus* | 17 | 15 | Alaska |
| *C. l. arctos* | 5 | 5 | Northwest Territories, Ellesmere Island |
| *C. l. tundarum* | 3 | 4 | Alaska |

because of biases in preservation. The weighted average is the sum across all tooth types of the product of the observed fracture frequency per tooth type and the proportion of the tooth row represented by that tooth type in a complete dentition. Differences in frequency of fracture were assessed with the Pearson chi-square statistic (with a continuity correction in the case of 2 × 2 comparisons), and 95% confidence intervals were calculated based on the binomial distribution [S13].

Table S4. Measurements Used in the Morphometric Analyses and Their Definitions

| Measurement | Definition |
|---|---|
| FL | Face length: distance from just behind the incisors to the distal margin of the hard palate. |
| PL | Palatine length: distance from just behind the incisors to the distal margin of the palatines (at the palatine-maxilla suture) |
| TPRL | Total premolar row length: distance from the mesial border of the upper first premolar to the distal border of the upper fourth premolar. |
| PW | Palate width: hard palate breadth anterior to the upper fourth premolar. |
| P4L | Upper carnassial length: maximum mesiodistal length. |
| P4W | Upper carnassial width: maximum buccolingual breadth of the blade (behind the protocone). |
| M1L | Upper first molar length: maximum mesiodistal length along the buccal margin. |
| M1W | Upper first molar width: maximum buccolingual breadth. |
| M2L | Upper second molar length: maximum mesiodistal length along the buccal margin. |
| M2W | Upper second molar width: maximum buccolingual breadth. |
| SD | Snout depth: maximum rostrum height just distal to the upper-canine-tooth alveolus. |
| dd | Dentary depth: maximum dorsoventral height just posterior to the lower-first-molar alveolus. |
| p4L | Lower fourth premolar length: maximum mesiodistal length. |
| m1L | Lower carnassial length: maximum mesiodistal length. |
| m1TRL | Lower carnassial blade length: maximum mesiodistal length of the trigonid of the lower first molar. |
| m1W | Lower carnassial width: maximum buccolingual breadth of the trigonid of the lower first molar. |
| m2L | Lower second molar length: maximum mesiodistal length. |
| m2W | Lower second molar width: maximum buccolingual breadth. |

### Stable-Isotope Analyses

As noted in the results, we collected $\delta^{13}C$ and $\delta^{15}N$ data from fossil bone collagen for wolves and their potential prey, including 32 horses (*Equus lambei*), ten caribou *(Rangifer tarandus*), six bison (*Bison bison*), five yak (*Bos grunniens*), and ten woodland muskox (*Symbos cavifrons*) from the Fairbanks area (Table S8). Also included are published $\delta^{13}C$ and $\delta^{15}N$ data collected from undated Pleistocene mammoths (*M. primigenius)* from multiple sites in Alaska [S14]. Thirty-two horses, ten caribou and 58 wolves were radiocarbon dated (Tables S1 and S8).

Bone samples (~150 mg) were crushed into coarse powder in a mortar and pestle, and collagen was extracted according to the methods of Brown et al. [S15]. Collagen preservation was assessed with atomic carbon/nitrogen (C/N) ratios, and all samples presented here were between 2.2:1 and 2.8:1, well within the range for viable collagen [S16]. For stable-isotope analyses, collagen samples (1.0 mg) were weighed into tin capsules. Carbon and nitrogen stable-isotope ratios were measured with an elemental analyzer coupled with a mass spectrometer (Europa Hydra 20/20) at the University of California Davis Stable Isotope Facility. Stable-isotope compositions are reported with standard $\delta$ notation and are referenced to Vienna PeeDee Belemnite and air for carbon and nitrogen, respectively. The standard deviation for replicates of a gelatin standard was <0.2‰ for carbon and nitrogen. Pleistocene collagen samples analyzed for radiocarbon were prepared with the same method outlined above. Because there is no agreed-upon calibration curve for $^{14}C$ ages >26 ka BP [S17], we present all dates as uncalibrated $^{14}C$ ages.

Because of climate driven change in isotope values, the $^{14}C$ dated wolves, horses, and caribou were grouped into three climatically relevant time periods: postglacial (18 to 10 ka BP), full-glacial (23 to 18 ka BP), and preglacial (>50 to 23 ka BP). The preglacial time period encompasses mild conditions that persisted until approximately 25 ka BP, followed by the onset of last glacial maximum (LGM) cooling. The full-glacial group captures the 5000 year period when LGM conditions were the coldest and driest in eastern Beringia, and the postglacial time period is characterized by a rapid transition toward the warmer, mesic conditions of the Holocene.

### Supplemental References


S1. Leonard, J., Wayne, R., and Cooper, A. (2000). Population genetics of ice age brown bears. Proc. Natl. Acad. Sci. USA *97*, 1651–1654.

S2. Leonard, J., Shanks, O., Hofreiter, M., Kreuz, E., Hodges, L., Ream, W., Wayne, R., and Fleischer, R. (2006). Animal DNA in PCR reagents plagues ancient DNA research. Journal of Archaeological Science. Published online December 5, 2006. 10.1016/j.jas.2006.10.023.

S3. Leonard, J.A., Vila, C., and Wayne, R.K. (2005). Legacy lost: Genetic variability and population size of extirpated US grey wolves (Canis lupus). Mol. Ecol. *14*, 9–17.

Table S5. Mean and Standard Deviations for Raw Measurements Used in the Bivariate and Multivariate Analyses of the Extant and Two Late Pleistocene Wolf Samples

| Measurement | Mean (SD) for Extant Wolves | Mean (SD) for Rancho La Brea Wolves | Mean (SD) for Beringian Wolves |
|---|---|---|---|
| Face length (FL) | 114.5 (7.36) | 115.8 (7.05) | 115.6 (4.97) |
| Palatine length (PL) | 73.4 (4.64) | 75.2 (5.16) | 73.9 (3.62) |
| Premolar row length (TPRL)* | 63.4 (4.32) | 63.6 (4.56) | 69.3 (3.69) |
| Palate width (PW)* | 64.9 (4.68) | 67.6 (2.06) | 76.6 (4.66) |
| P4 length (P4L)* | 25.1 (1.61) | 26.3 (2.01) | 26.7 (1.59) |
| P4 width (P4W) * | 10.1 (0.88) | 10.6 (0.65) | 11.35 (0.71) |
| M1 length (M1L) | 16.4 (1.07) | 16.5 (1.69) | 16.6 (0.84) |
| M1 width (M1W) | 22.2 (1.43) | 22.1 (1.51) | 22.1 (1.06) |
| M2 length (M2L)* | 8.7 (0.67) | 8.92 (0.54) | 9.2 (0.48) |
| M2 width (M2W) | 13.5 (1.01) | 13.8 (0.65) | 13.6 (0.84) |
| Snout depth (SD) | 42.6 (3.98) | 40.9 (2.86) | 43.5 (2.63) |
| dentary depth (dd)* | 30.4 (2.88) | 31.6 (0.53) | 32.7 (2.41) |
| p4 length (p4l)* | 15.4 (1.03) | 16.6 (1.64) | 16.5 (0.75) |
| m1 length (m1L)* | 28.2 (1.86) | 28.9 (2.26) | 29.6 (1.91) |
| m1 trigonid length (m1trl)* | 19.6 (1.49) | 21.9 (1.28) | 20.9 (1.43) |
| m1 width (m1w)* | 10.7 (0.85) | 11.3 (0.08) | 11.1 (0.86) |
| m2 length (m2l) | 11.7 (0.81) | 11.4 (1.12) | 11.6 (0.75) |
| m2 width (m2w) | 8.95 (0.62) | 8.39 (0.19) | 8.8 (0.63) |

For measurement definitions, see Table S4. "*" denotes eastern-Beringian samples that differ significantly ($p < 0.05$) from the other two (for cranial measurements) or from modern wolves (for dentary measurements).


S4. Vilà, C., Amorim, I.R., Leonard, J.A., Posada, D., Castroviejo, J., Petrucci-Fonseca, F., Crandall, K.E., Ellegren, H., and Wayne, R.K. (1999). Mitochondrial DNA phylogeography and population history of the grey wolf Canis lupus. Mol. Ecol. *8*, 2089–2103.

S5. Sharma, D.K., Maldonado, J.E., Jhala, Y.V., and Fleischer, R.C. (2003). Ancient wolf lineages in India. Proc. R. Soc. Lond. B. Biol. Sci. *271*, S1–S4.

S6. Rozas, J., Sanchez-DelBarrio, J.C., Messeguer, X., and Rozas, R. (2003). DnaSP, DNA polymorphism analyses by the coalescent and other methods. Bioinformatics *19*, 2496–2497.


Table S6. Results of Principal Components Analysis

| Shape Variable | Factor 1 | Factor 2 |
|---|---|---|
| *Crania* | | |
| M2W | −0.764 | 0.141 |
| TPRL | 0.755 | −0.217 |
| M2L | −0.624 | −0.004 |
| PW | 0.617 | −0.529 |
| M1L | −0.588 | 0.104 |
| M1W | −0.58 | 0.361 |
| SD | 0.408 | 0.354 |
| FL | 0.474 | 0.769 |
| P4W | −0.004 | −0.707 |
| PL | 0.473 | 0.672 |
| P4L | −0.109 | −0.39 |
| % variance | 29.4 | 21 |
| *Dentaries* | | |
| m2W | −0.891 | 0.116 |
| m2L | −0.853 | 0.007 |
| m1TR | 0.718 | 0.319 |
| m1L | 0.568 | 0.516 |
| dh | 0.488 | −0.716 |
| m1W | 0.222 | 0.519 |
| p4L | 0.351 | −0.357 |
| % variance | 39.6 | 18.5 |

Variable loadings and percent variance explained on the first two axes of a principal-components analysis of the $\log_{10}$-transformed shape variables for the cranial and dentary samples, respectively. For variable abbreviations, see Table S5.


S7. Swofford, D.L. (2002). PAUP*. Phylogenetic Analysis Using Patsimony (*And Other Methods), Version 4.0b10 (Sunderland, Massachusetts: Sinauer Associates).

S8. Posada, D., and Crandall, K.A. (1998). MODELTEST: Testing the model of DNA substitution. Bioinformatics *14*, 817–818.

S9. Mosimann, J.E., and James, F.C. (1979). New statistical methods for allometry with application to Florida red-winged blackbirds. Evolution Int. J. Org. Evolution *33*, 444–459.

S10. Jungers, W.L., Falsetti, A.B., and Wall, C.E. (1995). Shape, relative size, and size adjustments in morphometrics. Yearb. Phys. Anthropol. *38*, 137–162.

S11. Van Valkenburgh, B., and Hertel, F. (1993). Tough times at La Brea: Tooth breakage in large carnivores of the late Pleistocene. Science *261*, 456–459.

S12. Van Valkenburgh, B. (1988). Incidence of tooth breakage among large, predatory mammals. Am. Nat. *131*, 291–302.

S13. Wonnacott, R., and Wonnacott, T. (1985). Introductory Statistics, Fourth Edition (New York: Wiley).

S14. Bocherens, H., Fizet, M., Mariotti, A., Gangloff, R.A., and Burns, J.A. (1994). Contribution of isotopic biogeochemistry (13C, 15N, 18O) to the paleoecology of mammoths (*Mammuthus primigenius*). Historical Biology *7*, 187–202.

S15. Brown, T.A., Nelson, D.E., Vogel, J.S., and Southon, J.R. (1988). Improved collagen extraction by modified Longin method. Radiocarbon *30*, 171–177.

S16. Ambrose, S.H. (1990). Preparation and characterization of bone and tooth collagen for isotopic analysis. J. Archaeol. Sci. *17*, 431–451.

S17. Reimer, P.J., Baillie, M.G.L., Bard, E., Beck, J.W., Blackwell, P.G., Buck, C.E., Burr, G.S., Edwards, R.L., Guilderson, M.F.T.P., Hogg, A.G., et al. (2006). Comment on "Radiocarbon calibration curve spanning 0 to 50,000 years BP based on paired 230Th/234U/238U and 14C dates on pristine corals" by R.G. Fairbanks et al. (Quaternary Science Reviews 24 (2005) 1781–1796) and "Extending the radiocarbon calibration beyond 26,000 years before present using fossil corals" by T.-C. Chiu et al. (Quaternary Science Reviews 24 (2005) 1797–1808). Quaternary Science Reviews *25*, 855–862.

Table S7. Observed Number of Total and Broken Teeth in Four Historical and One Pleistocene Eastern-Beringian Wolf Populations

| Population | Provenance | n (skulls) | Total Teeth (No.) | Broken Teeth (No.) | Fracture Frequency | |
|---|---|---|---|---|---|---|
| | | | | | With Incisors | Without Incisors |
| *C. l. lycaon* | Minnesota, Michigan | 90 | 2955 | 193 | 0.07 (0.009) | 0.07 (0.009) |
| *C.l. irremotus* | Canada, Idaho | 66 | 2459 | 48 | 0.02 (0.007) | 0.01 (0.009) |
| *C. l. nubilis* | New Mexico, Texas | 83 | 3250 | 123 | 0.04 (0.009) | 0.05 (0.009) |
| *C. l. pambasileus* | Alaska | 74 | 2910 | 125 | 0.04 (0.009) | 0.05 (0.01) |
| *C. lupus* | Eastern Beringia | 37[a] | 373 | 36 | 0.11 (0.04) | 0.1 (0.04) |

Fracture frequency is equal to the weighted average of tooth-breakage frequencies for each tooth type (incisors, canines, premolars, carnassials, and molars). See Supplemental Experimental Procedures for further explanation. Shown in parentheses are ± 95% confidence intervals for the fracture frequencies.

[a] For the Pleistocene sample, n is the total number of specimens (lower jaws and skulls).

Table S8. List of Fossil Specimens Used in the Stable Isotope Analyses and Their Radiocarbon Dates

| Species | Specimen ID | $\delta^{13}C$ | $\delta^{15}N$ | $^{14}C$ Age | Lab ID |
|---|---|---|---|---|---|
| *Clu* | AMNH FM 30450 | −19.4 | 5.6 | | AA48695 |
| *Clu* | AMNH FM 70944 | −19.2 | 7.3 | | AA38449 |
| *Clu* | AMNH FM 30447 | −19.7 | 7.9 | | AA35223 |
| *Clu* | AMNH FM 67227 | −18.9 | 7.9 | | AA35231 |
| *Clu* | AMNH FM 68009-A | −18.9 | 8.0 | | AA35227 |
| *Clu* | AMNH FM 67224 | −19.0 | 7.8 | | AA35226 |
| *Clu* | AMNH FM 30432 | −20.5 | 8.1 | | AA48704 |
| *Clu* | AMNH FM 30453 | −18.3 | 9.3 | | AA48702 |
| *Clu* | AMNH FM 70942 | −19.8 | 9.3 | | CAMS115775 |
| *Clu* | AMNH FM 30452 | −19.1 | 9.1 | | CAMS115769 |
| *Clu* | AMNH FM 67231 | −19.3 | 9.3 | | CAMS115774 |
| *Clu* | AMNH FM 68008-G | −19.2 | 8.5 | | AA35222 |
| *Clu* | AMNH FM 67170 | −18.3 | 7.3 | | AA48694 |
| *Clu* | AMNH FM 30431 | −19.1 | 8.6 | | CAMS115776 |
| *Clu* | AMNH FM 67248 | −19.7 | 6.2 | | CAMS115773 |
| *Clu* | AMNH FM 67168 | −19.0 | 9.2 | | CAMS115767 |
| *Clu* | AMNH FM 67163 | −18.8 | 6.6 | | AA48693 |
| *Clu* | AMNH FM 67228 | −19.4 | 7.0 | | AA42302 |
| *Clu* | NMC 42388 | −18.5 | 8.5 | | AA35221 |
| *Clu* | AMNH FM 67184 | −20.2 | 6.2 | | CAMS115763 |
| *Clu* | AMNH FM 67159 | −19.4 | 8.1 | | AA48703 |
| *Clu* | AMNH FM 70958 | −19.1 | 7.5 | | AA37615 |
| *Clu* | AMNH FM 70945 | −18.8 | 6.7 | | AA38448 |
| *Clu* | AMNH FM 67202 | −19.2 | 6.8 | | AA35224 |
| *Clu* | AMNH FM 67243 | −20.1 | 6.2 | | CAMS115772 |
| *Clu* | AMNH FM 67197 | −20.3 | 5.7 | | CAMS115760 |
| *Clu* | AMNH FM 67208 | −19.2 | 9.7 | | CAMS115759 |
| *Clu* | AMNH FM 30438 | −19.4 | 6.4 | | CAMS115778 |
| *Clu* | AMNH FM 67167 | −19.0 | 9.2 | | CAMS115768 |
| *Clu* | AMNH FM 67235 | −19.8 | 5.8 | | AA42310 |
| *Clu* | AMNH FM 70946 | −20.0 | 5.4 | | AA42313 |
| *Clu* | AMNH FM 30440 | −18.9 | 6.4 | | AA42314 |
| *Clu* | AMNH FM 142410 | −19.4 | 6.2 | | CAMS115762 |
| *Clu* | AMNH FM 142409 | −19.4 | 8.6 | | CAMS115777 |
| *Clu* | AMNH FM 67165 | −19.2 | 8.6 | | AA42317 |
| *Clu* | AMNH FM 67157 | −18.7 | 7.9 | | AA42315 |
| *Clu* | AMNH FM 30451 | −18.6 | 8.8 | | UCR 3761 |
| *Clu* | AMNH FM 67169 | −19.3 | 10.3 | | AA35216A |
| *Clu* | NMC 9929 | −19.3 | 12.7 | | UCR 3764 |
| *Clu* | NMC 17311 | −19.1 | 6.1 | | UCR 3762 |
| *Eq* | AMNH FM 60003 | 1.41 | −21.25 | 24260 ± 200 | CAMS120077 |
| *Eq* | AMNH FM 60004 | 3.08 | −20.93 | 16370 ± 80 | CAM119968 |
| *Eq* | AMNH FM 60005 | 1.64 | −21.29 | 14630 ± 60 | CAMS119969 |
| *Eq* | AMNH FM 60044 | 3.47 | −20.85 | 18630 ± 100 | CAMS119970 |
| *Eq* | AMNH FM 142419 | 4.52 | −21.07 | 20520 ± 120 | CAMS119971 |
| *Eq* | AMNH FM 60017 | 3.58 | −21.58 | 41000 ± 1500 | CAMS119972 |
| *Eq* | AMNH FM 142420 | 4.96 | −21.23 | 19870 ± 110 | CAMS119973 |
| *Eq* | AMNH FM 142421 | 4.79 | −20.95 | 14860 ± 60 | CAMS119974 |
| *Eq* | AMNH FM 142422 | 2.98 | −21.50 | >48500 | CAMS119975 |

Table S8. *Continued*

| Species | Specimen ID | $\delta^{13}C$ | $\delta^{15}N$ | $^{14}C$ Age | Lab ID |
|---|---|---|---|---|---|
| *Eq* | AMNH FM 142423 | 3.85 | −20.90 | 12560 ± 50 | CAMS119976 |
| *Eq* | AMNH FM 142424 | 2.94 | −20.70 | 15460 ± 70 | CAMS119977 |
| *Eq* | AMNH FM 142425 | 4.23 | −20.76 | 20440 ± 120 | CAMS119978 |
| *Eq* | AMNH FM 142426 | 5.07 | −21.20 | 20300 ± 120 | CAMS119979 |
| *Eq* | AMNH FM 142427 | 4.73 | −21.05 | 19960 ± 110 | CAMS119980 |
| *Eq* | AMNH FM 142428 | 3.74 | −21.03 | 21280 ±130 | CAMS119981 |
| *Eq* | AMNH FM 142429 | 4.29 | −21.28 | 12310 ± 45 | CAMS119982 |
| *Eq* | AMNH FM 142430 | 3.23 | −21.40 | 19950 ± 110 | CAMS119983 |
| *Eq* | AMNH FM 60019 | 1.65 | −21.50 | >48500 | CAMS119984 |
| *Eq* | AMNH FM 142431 | 3.94 | −21.09 | 25710 ± 230 | CAMS119985 |
| *Eq* | AMNH FM 142432 | 2.47 | −21.48 | 48500 | CAMS119986 |
| *Eq* | AMNH FM 142433 | 2.85 | −20.70 | 25960 ± 240 | CAMS119987 |
| *Eq* | AMNH FM 142434 | 3.76 | −20.97 | 22610 ± 150 | CAMS119988 |
| *Eq* | AMNH FM 142435 | 3.82 | −21.87 | 21840 ± 140 | CAMS119989 |
| *Eq* | AMNH FM 60023 | 2.53 | −21.45 | 19000 ± 100 | CAMS120058 |
| *Eq* | AMNH FM 60027 | 3.60 | −20.81 | 19590 ± 110 | CAMS120059 |
| *Eq* | AMNH FM 60026 | 3.96 | −21.32 | 21310 ± 140 | CAMS120060 |
| *Eq* | AMNH FM 60025 | 4.65 | −21.19 | 13710 ± 60 | CAMS120061 |
| *Eq* | AMNH FM 60020 | 3.99 | −21.25 | 19950 ± 120 | CAMS120062 |
| *Eq* | AMNH FM 60028 | 4.43 | −20.63 | >48400 | CAMS120064 |
| *Eq* | AMNH FM 60221 | 0.74 | −21.70 | 43700 ± 2000 | CAMS120067 |
| *Eq* | AMNH FM 60032 | 2.54 | −20.89 | 15850 ± 70 | CAMS120068 |
| *Eq* | AMNH FM 60033 | 2.64 | −20.87 | 39910 ± 1330 | CAMS120069 |
| *Rta* | AMNH FM 142438 | 3.63 | −20.08 | 21142 ± 361 | AA48680 |
| *Rta* | AMNH FM 142439 | 1.97 | −19.45 | 16721 ± 207 | AA48682 |
| *Rta* | AMNH FM 142440 | 5.43 | −20.07 | 17287 ± 222 | AA48683 |
| *Rta* | AMNH FM 142441 | 3.26 | −19.21 | 16070 ± 190 | AA48686 |
| *Rta* | AMNH FM 142442 | 3.13 | −18.99 | 16420 ± 202 | AA48687 |
| *Rta* | AMNH FM 142443 | 2.13 | −19.27 | >40707 | AA48681 |
| *Rta* | AMNH FM 142444 | 4.67 | −19.43 | >40673 | AA48685 |
| *Rta* | AMNH FM 142445 | 3.65 | −19.72 | >41100 | AA48688 |
| *Rta* | AMNH FM 142446 | 3.13 | −19.31 | 29640 ± 370 | CAMS120070 |
| *Rta* | AMNH FM 142447 | 1.69 | −19.19 | >45200 | CAMS120071 |
| *Bbi* | AMNH FM 5092 | 4.38 | −20.08 | | |
| *Bbi* | AMNH FM 46555 | 5.21 | −20.10 | | |
| *Bbi* | AMNH FM 46858 | 3.73 | −20.88 | | |
| *Bbi* | AMNH FM 46856 | 2.93 | −19.77 | | |
| *Bbi* | AMNH FM 3135 | 5.22 | −20.51 | | |
| *Bbi* | AMNH FM 1636 | 4.38 | −21.34 | | |
| *Bos* | AMNH FM 142448 | 2.65 | −20.73 | | |
| *Bos* | AMNH FM 142449 | 0.47 | −24.16 | | |
| *Bos* | AMNH FM 142450 | 0.98 | −20.38 | | |
| *Bos* | AMNH FM 142451 | 4.77 | −21.68 | | |

The following species abbreviations are used: *Canis lupus* (*Clu*), *Equus lambei* (*Eq*), *Rangifer tarandus* (*Rta*), *Bison bison* (*Bbi*), *Bos grunniens* (*Bos*), and *Symbos cavifrons* (*Sca*). Museum and radiocarbon dating laboratory abbreviations are as in Table S1. Radiocarbon dates for the wolf specimens are in Table S1. Methods: Collagen samples (1.0 mg) were weighed into tin capsules. Carbon and nitrogen stable-isotope ratios were measured with an elemental analyzer coupled with a mass spectrometer (Europa Hydra 20/20) at the University of California Davis Stable Isotope Facility. Stable-isotope compositions are reported with standard $\delta$ notation and are referenced to Vienna PeeDee Belemnite and air for carbon and nitrogen, respectively. The standard deviation for replicates of a gelatin standard was <0.2‰ for carbon and nitrogen.